ELSEVIER

Int. J. of Refractory Metals & Hard Materials **15** (1997) 65–71

0263-4368/97/$17.00

PII: S0263-4368(96)00014-5

The Relationship Between Electrochemical Behaviour and In-service Corrosion of WC Based Cemented Carbides

A. M. Human* & H. E. Exner

Institute of Physical Metallurgy, Faculty of Materials Science, Technical University of Darmstadt, Petersenstr. 30, 64287 Darmstadt, Germany

(Received 31 October 1995; accepted 13 February 1996)

Abstract: In long-life applications, the corrosion properties of cemented carbides can have a large influence on overall performance. Cemented carbides with improved corrosion resistance have been developed and are now commercially available. The understanding of the corrosion behaviour has been mostly empirical and satisfying explanations of the relationship between the electromechanical behaviour and in-service corrosion have been lacking.

In this paper, the electromechanical behaviour of WC–Co is modelled using the behaviour of pure WC and Co(W,C) alloys, according to a linear rule of mixtures. By comparing WC–Co with WC–Ni(Cr,Mo) in both normal sulphuric acid and a synthetic mine water, it is shown that the behaviour of the two grades is inherently different. WC–Co exhibits a 'pseudo-passivity' during electromechanical tests but corrodes actively in industrial applications. In contrast, WC–Ni(Cr,Mo) passivates and the rate of corrosion can be several orders of magnitude lower than that of WC–Co. © 1997 Elsevier Science Limited

1 INTRODUCTION

A considerable amount of research has been concerned with the corrosion of cemented carbides, but this has been largely limited to comparisons of corrosion rates in different solutions, using weight loss measurements. There have been a few studies aimed at understanding the processes involved and these have all made use of electromechanical measurements.[1–8]

Since the cobalt binder phase is most susceptible to corrosion in acidic media, it follows that improvement of the corrosion resistance of the binder will have a major influence on the overall corrosion resistance. As a result, researchers have substituted cobalt with nickel, nickel–chromium and nickel–cobalt binders and have generally reported a reduction in corrosion.[2,9,10]

Only more recently it has been shown that the electromechanical behaviour of WC–Co composites can be modelled using a simple linear rule of mixtures.[11,12]

$$i^{WC-Co} = A_A^{WC} \cdot i^{WC} + A_A^{Co} \cdot i^{Co} \quad (1)$$

where i^{WC-Co} is the electrochemical current density of the WC–Co composite, A_A^{WC} is the cross-sectional area fraction of the WC phase, i^{WC} is the current density of WC, A_A^{Co} is the cross-sectional area fraction of the binder phase and i^{Co} is the current density of a Co(W,C) alloy, representative of the binder composition.

The aim of this paper is to relate the electromechanical behaviour of cemented carbide composites to their in-service corrosion behaviour. Additionally, the influence of binder sub-

*Present address: DEBEX (Pty) Ltd, PO Box 11178, 1567 Selcourt, Gauteng, South Africa.

stitution on the corrosion behaviour is determined.

2 EXPERIMENTAL

All the cemented carbide specimens were produced using conventional powder metallurgical techniques. The amount of dissolved tungsten in the binder after conventional liquid phase sintering was determined using the magnetic properties of the alloys.[11] The average tungsten content of the binder is calculated to be 4 wt% (1·33 at%) and, according to the measurements of Hellsing,[13] the amount of carbon dissolved in the binder of conventionally sintered cemented carbides is below 0·02 wt% (0·1 at%). The microstructures were characterised using well established stereological parameters determined by lineal analysis.[14]

In order to study the effects of binder content and WC grain size on the electrochemical behaviour of cemented carbides, a range of composites were tested. The binder content was varied (6 and 17 wt%) with a constant WC average grain size ($\approx 2\ \mu m$). Conversely, the binder content was held constant (10 wt%) while the grain size was varied (≈ 1 and $5\ \mu m$). The effect of the binder composition on the electrochemical behaviour was examined using a WC–Ni(Cr,Mo) composite, the processing details of which are described in Human.[15] The binder content and WC grain size of the composites are given in Table 1.

The electrochemical behaviour of the cobalt binder phase is different to that of pure cobalt.[12,16] Therefore, the binder behaviour is approximated by a Co(W,C) alloy of similar composition to that of the binder after liquid phase sintering. A Co(W,C) alloy containing 4 wt% tungsten and less than 0·002 wt% carbon is used here to model the binder phase. A description of the manufacturing process and properties of this alloy are given in Roebuck & Almond.[17] Hot-pressed WC is used to model the WC phase.

Table 1. Composition and grain size of alloys investigated

Composite	*Binder content (wt%)*	*Average WC grain size (μm)*
M6	6	2
M17	17	2
F10	10	1
C10	10	5
Ni6	6	1

Table 2. Synthetic mine water composition[18]

Compound	*Concentration (mg l^{-1})*
Na_2SO_4	1237
$CaCl_2$	1038
$MgSO_4$	199
NaCl	1380

The electrochemical experiments were conducted in both 1N H_2SO_4 and a synthetic mine water solution (as used by Allen).[18] The composition of the synthetic mine water solution is given in Table 2. Measurements were performed using a standard three electrode cell. A saturated calomel electrode (SCE=SHE-241 mV) was used as a reference electrode and a platinum gauze as the counter electrode. All potentials are reported vs the SCE. The electrolyte was agitated and deaerated with ultra-high purity nitrogen gas (99·996%). The test surface of the WC and hardmetal specimens was approximately 1 cm^2 and of the cobalt alloy specimens approximately 0·2 cm^2. Specimens were polarised to −800 mV for 10 min, allowed to stabilise for one hour and then polarised in a positive direction at a scan rate of 0·2 mV s^{-1}.

Microstructural changes during corrosion were examined by polarising specimens for short lengths of time (between 1 and 20 min) and the identical position (marked by diamond indentation) compared with the polished surface using a scanning electron microscope (SEM). Film formation was examined by light abrasion of the specimen surface during the electrochemical tests.

3 RESULTS

3.1 WC–Co composites

In Table 3 typical electrochemical parameters for the alloys tested are listed, including the corrosion potential, E_{corr}, the primary passivation potential, E_{pp} and the critical current density, i_{cc}.

In Fig. 1 the weighted (i.e area fraction × current density) polarisation curves of WC and the

Table 3. Electrochemical corrosion parameters

Alloy	E_{corr} *mV*	E_{pp} *mV*	i_{cc}^{Co} *mA cm* $^{-2}$
Co(W,C)	−325	−50	156
WC	−150	—	—
F10	−330	−80	147
M6	−330	−80	126
M17	−320	−50	174
C10	−321	−54	141
Ni6	−200	−40	3

Co(W,C) alloy are compared with the polarisation behaviour of a WC–Co composite in 1N H_2SO_4. Initially, with increasing polarisation, the corrosion current of the WC–Co composite results almost exclusively from oxidation of the binder phase at the lower potentials. The partial current due to binder phase oxidation initially increases exponentially with increasing potential. A maximum is reached after which the current abruptly decreases. Thereafter the current density appears to remain relatively independent of the applied potential. Although this is phenomenologically similar to passive behaviour, the form of the polarisation curve has been shown to be due to an ohmic drop at the specimen surface, caused by a thick surface deposit.[12,16] The magnitude of the current density remains extremely high (around 50 mA cm^{-2}) in comparison to passive current densities (below 10 μA cm^{-2}) and the region has been termed pseudo-passive.[12,16] At around 250 mV the partial current due to WC oxidation becomes visible and increases with increasing potential. The WC partial current only becomes significant above around 750 mV where the

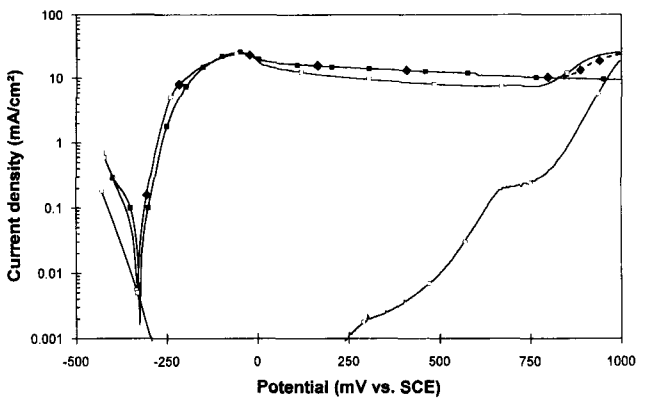

Fig. 1. Polarisation curves across entire potential range: (○) weighted WC, (■) weighted Co(W,C) alloy (□) M10 composite, (♦) predicted by model.

WC–Co current density increases above that of the Co(W,C) alloy. This rise is also similar to typical transpassive behaviour and only through comparison with the individual phases has it become apparent that the current increase is due to WC oxidation and not to a surface film breakdown.

A notable difference in behaviour between the Co(W,C) alloy and the WC–Co composites is observed in the pseudo-passive regime. Light abrasion of a Co(W,C) specimen results in a sharp increase in the current density but has no effect on WC–Co specimens. This is because the surface of the binder phase is protected by the WC network, which is raised above the binder surface at this stage of the oxidation process. The preferential attack of the binder phase is seen in micrographs comparing the polished surface with a corroded surface. In Fig. 2(a) a SEM micrograph of a WC–Co composite polished surface is shown. The same area, after corrosion at the corrosion potential, E_{corr}, is shown in Fig. 2(b). The surface area of the binder phase corrodes preferentially to the carbide phase. The binder phase corrodes by a pitting mechanism and attack at the carbide/binder interfaces is exaggerated. The binder region adjacent to the corners of WC grains is notably attacked and this is especially the case where the meeting of two WC grains forms an acute angle in the binder phase. This may be due to higher tensile stresses in such regions of the binder due to thermal mismatch, as reported by Spiegler *et al.*[19] In region A, marked on the figures, it can be seen how a WC grain, initially covered by the binder, is revealed by binder removal. The sharp edges of the WC grains after corrosion highlight the inert nature of the WC phase at this potential.

As shown above, the measured current density stems almost exclusively from oxidation of the binder phase, especially at low potentials. Therefore it can be expected that as the binder content is increased, the corrosion current will increase proportionally. In previous literature,[1–8] the current density has been calculated using the full exposed surface area, i.e. the WC area plus the binder area. Taking the full WC–Co area into account results in the erroneous trend of increasing corrosion current density with increasing binder content, Fig. 3(a). In Fig. 3(b) the polarisation behaviour of the same composites is depicted, but in this case the cur-

rent densities have been calculated using only the area fraction of the binder phase. There is no significant difference in the magnitude of the anodic current densities indicating that an increase in the corrosion rate with increasing binder content is due only to an increase in area fraction of the binder phase.

A change in the WC grain size does not result in any measurable difference in the polarisation behaviour, as shown in Fig. 4. There is no significant difference between the polarisation curves with a change in the average WC grain size from 1 to 5 μm.

In synthetic mine water the corrosion potential of a WC–Co composite is markedly shifted to a more negative value ($E_{corr} \approx -600$ mV) as shown in Fig. 5. The current density increases with increasing polarisation and at around -200 mV the current density coincides with that measured in sulphuric acid and remains similar at higher potentials. The pseudo-passivation is not as pronounced as in sulphuric acid.

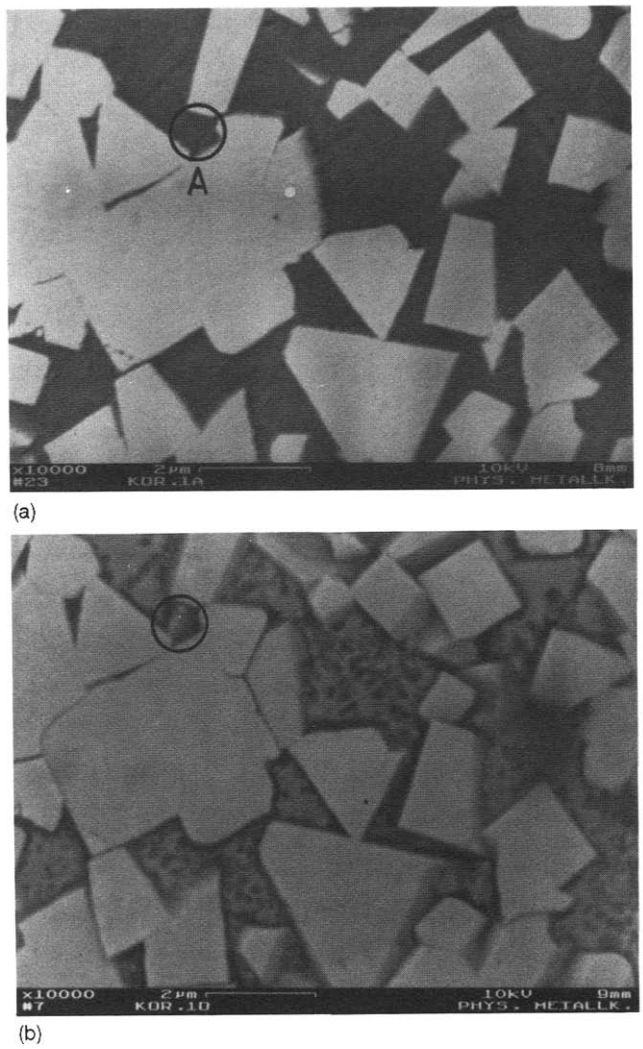

Fig. 2. SEM micrographs of the surface of a WC–Co composite. The dark area is the cobalt based binder and the light areas WC: (a) polished surface, (b) after 10 min polarisation at -250 mV in 1 N H_2SO_4.

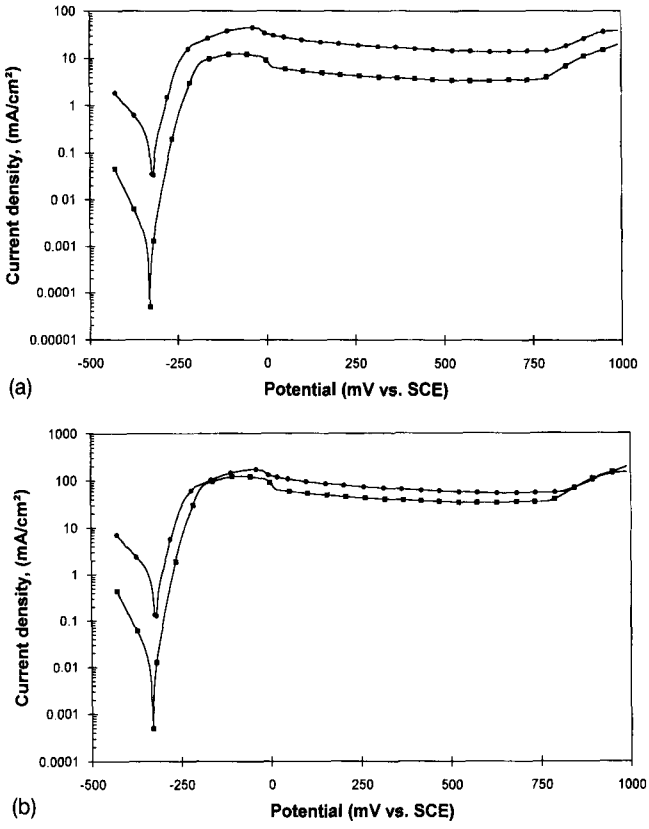

Fig. 3. Full polarisation scans for composites M6 (■) and M17 (●): (a) current calculated taking the full area into account (i^{WC-Co}), (b) current calculated taking only the binder area into account (i^{Co}).

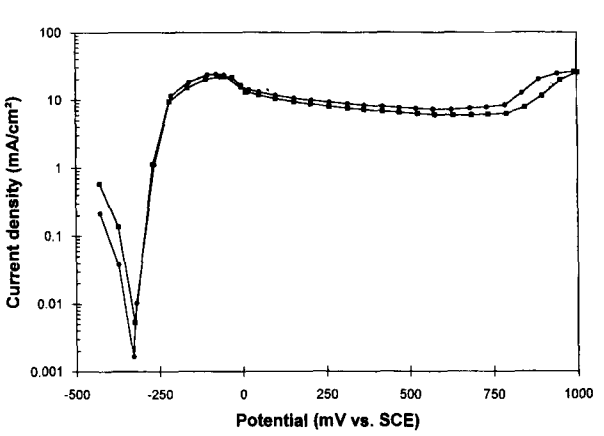

Fig. 4. Polarisation scans of WC–Co composites with equal binder contents (10 wt%), and (●) fine 1 μm, or (■) coarse 5 μm, WC grain size.

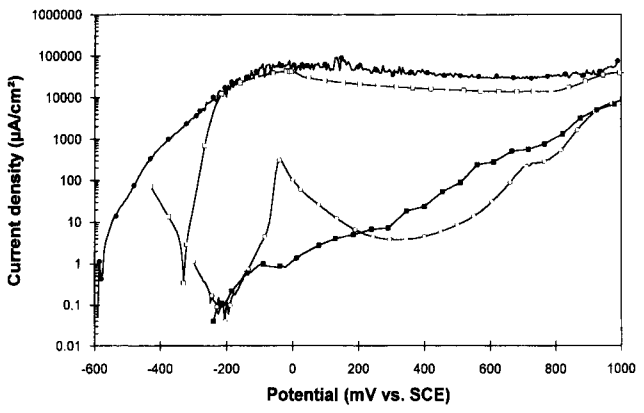

Fig. 5. Potentiodynamic polarisation scans of WC–Co (□), (●) and WC–Ni(Cr,Mo) (○), (■), in 1N H_2SO_4 (open symbols) and synthetic mine water (closed symbols) respectively.

3.2 WC–Ni(Cr,Mo) composite

In Fig. 6 the polarisation behaviour of a hardmetal with a nickel based binder (F6Ni) in 1N H_2SO_4 is compared with that of a conventional cobalt binder composite (M6) and pure WC. Both hardmetals have a 6 wt% (10 vol%) binder content and accordingly the current density of the pure WC has been weighted to take the WC area fraction in the cemented carbides into account, i.e.

$$i^{WC}_{weighted}=A^{WC}_{A}\frac{I^{WC}}{A^{WC}}=0{\cdot}9i^{WC} \qquad (2)$$

where A^{WC}_{A} is the WC area fraction in the WC–Co composite, A^{WC} is the exposed surface area of the pure WC specimen, I^{WC} is the measured electrochemical current of the WC specimen and i^{WC} is the current density. The nickel based binder composite has a corrosion potential ($E_{corr}\approx -200$ mV) noble to that of the cobalt binder composites ($E_{corr}=-330$ mV). The cathodic Tafel slope and exchange current density of F6Ni are identical to that of the weighted WC, indicating that the cathodic current predominantly originates from the WC surface. At potentials positive to E_{corr} the current density increases exponentially indicating activation control. At −40 mV the primary passivation potential, E_{pp}, is reached and the current sharply drops. The current density reaches a minimum of approximately 4 μA cm^{-2} at 300 mV. As the potential is increased above 300 mV the current density gradually rises. From the weighted current density of the pure WC it is clear that the rise is due to the proportion of current arising from the oxidation of WC. With increasing potential, the polarisation behaviour closely resembles that of pure WC.

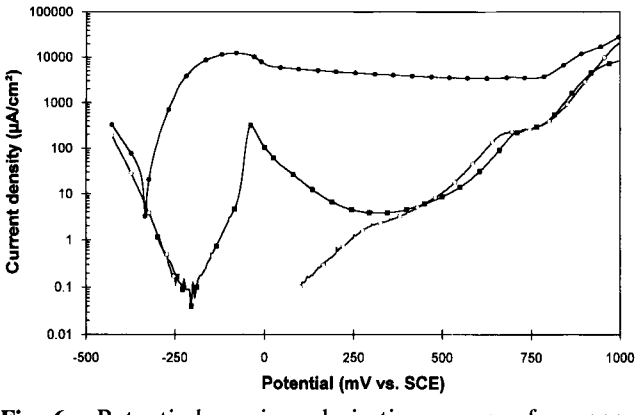

Fig. 6. Potentiodynamic polarisation curve of composites F6Ni (■), M6 (●) and the weighted curve of pure WC (○) in 1N H_2SO_4.

It is well known that true passive currents of Ni–Cr stainless steel may take several hours to be achieved and therefore, in order to determine the full extent of passivation which occurs for F6Ni, a specimen was held at 300 mV for approximately 17 hours and the current recorded. The current density stabilised at a minimum value of approximately 1·5 μA cm^{-2}.

In synthetic mine water the nickel based binder composite shows no change in the anodic and cathodic reaction kinetics at the corrosion potential (Fig. 5). The anodic and cathodic Tafel slopes and exchange current densities are similar to those measured in sulphuric acid and hence E_{corr} is unchanged. A significant change is the reduction in the critical current density in synthetic mine water. The nickel based binder composite passivates at approximately −100 mV with $i_{cc}=1$ μA cm^{-2}, 400 times lower than that in 1N H_2SO_4. The current immediately begins to rise after passivation and by comparison with the behaviour of pure WC it is apparent that this is due to the oxidation of WC (see Fig. 6).

4 DISCUSSION

4.1 Influence of binder substitution and the electrolyte

Because the corrosion behaviour of WC–Co composites is almost exclusively defined by the

properties of the binder phase, binder substitution results in striking changes. Substituting the conventional cobalt binder with a more corrosion resistant Ni(Cr,Mo) binder significantly reduces the current density. The nickel based binder composite is more noble than cobalt and the Tafel slope is lower, the combination of which results in an active corrosion current density, i_{corr}, which is up to 600 times lower than that of the WC–Co composites. This is in agreement with the standard potentials for cobalt oxidation ($E°=-518$ mV) and nickel oxidation ($E°=-491$ mV).

The behaviour of the WC–Ni(Cr,Mo) composite after reaching a critical current density, i_{cc}, is fundamentally different to that of the WC–Co composites (Fig. 6). The current density drops sharply to a minimum of approximately 4 μA cm^{-2}. At 300 mV the passive current density of Ni6 is more than 1000 times lower than the pseudo-passive current of M6. At this point the current due to oxidation of the nickel based binder phase is so low that current due to WC oxidation becomes proportionally high. The rise in current density with increasing potential is due to WC oxidation.[20]

$$WC+5H_2O=WO_3+CO_2+10H^++10e^- \quad (3)$$

The current density dropped to 1·5 μA cm^{-2} after holding at 300 mV for several hours. From Fig. 6 this can be seen to be equal to the current density of the pure WC and it can be concluded that the current density due to the binder phase drops to a value which is negligible in comparison. Thus, unlike the cobalt binder, the nickel based binder forms a true passive film which hinders further oxidation.

Tests in synthetic mine water highlighted further differences between the cobalt and nickel based binders (Fig. 5). The synthetic mine water solution had a neutral pH (6) and a high concentration of ions, especially chloride ions. The change in electrolyte had very little influence on the polarisation behaviour of the WC–Co composite, resulting only in a negative shift of E_{corr} and higher pseudo-passive currents (Fig. 5). In contrast, the change in electrolyte resulted in a pronounced drop in the critical current density of the WC–Ni(Cr,Mo) composite from around 300 μA cm^{-2} to 1 μA cm^{-2}. The lower current due to binder oxidation results in the WC oxidation current becoming prominent at lower potentials. The drop in i_{cc} with increasing pH is in accordance with that found for Ni–Cr alloys.[21]

4.2 Application to practical corrosion problems

Most electrochemical investigations of the system WC–Co[1–8] have failed to recognise that the magnitudes of the critical and passive currents are so high as to have no practical significance when free corroding systems are considered. The results of this work show that the corrosion currents up to around 800 mV are primarily due to cobalt oxidation. The true critical current density, i_{cc}^{Co}, i.e. taking only the sectional binder area into account, is at least 130 mA cm^{-2} and the true pseudo-passive current density, i_p^{Co}, at least 50 mA cm^{-2}. The critical current density is at least 1000 times higher than the maximum cathodic current density (100 μA cm^{-2}) which can be provided by an aerated solution with a pH around 7.[21] The pseudo-passive current density is also much higher than 100 μA cm^{-2}. In effect, this means that all the composites will remain active under free corroding conditions and the maximum corrosion rate will be fixed by the cathodic reaction (concentration polarisation).

The electrochemical equipment used in this work reduced the degree of experimental error to a minimum but the differences in the active corrosion rates of the composites remain within the experimental error. There is no significant change in the corrosion rate of the binder phase with varying binder content or WC grain size. Obviously the rate of material loss will increase with increasing binder content because the fraction of corroding phase is increased, but the kinetics of the binder phase corrosion are not measurably altered.

In comparison to the WC–Co composites, the composite with a Ni(Cr,Mo) binder has a reduced active corrosion rate and the ability to passivate. If the current densities are taken with respect to the binder surface area, i^{Ni}, then the WC–Ni(Cr,Mo) composite passivates in 1N H_2SO_4 with a critical current density of 3 mA cm^{-2}, which is also higher than expected cathodic currents in oxygenated aqueous environments. However, unlike WC–Co composites which show no change, increasing the pH results in a pronounced drop in the critical current density, i_{cc}^{Ni}, to about 10 μA cm^{-2}. Thus the WC–Ni(Cr,Mo) composite is self-passivating in

this environment. In typical industrial environments nickel based binder composites will have much lower corrosion rates while cobalt binders will corrode in the active state, with a corrosion rate largely controlled by the cathodic kinetics.

ACKNOWLEDGEMENTS

It is gratefully acknowledged that this work has been sponsored by De Beers Diamond Research Laboratory, Johannesburg, South Africa, the Foundation for Research Development (FRD), Pretoria, South Africa and the Deutscher Akademischer Austauschdienst (DAAD), Bonn, Germany.

REFERENCES

1. Ghandehari, M. H., Anodic behaviour of cemented WC–6%Co alloy in phosphoric acid solutions. *J. Electrochem. Soc.*, **127** (1980) 2144–7.
2. Ekemar, S., Lindholm, L. & Hartzell, T., Nickel as a binder in WC-based cemented carbides. *Int. J. Refr. Metals Hard Mater.*, **1** (1982) 37–40.
3. zur Megede, D. & Heitz, E., Das Korrosionsverhalten von Hartmetall-Verbundwerkstoffen in chloridhaltigen wäßrigen Lösungen. *Werkst. Korros.*, **37** (1986) 207–14.
4. Tomlinson, W. J. & Linzell, C. R., Anodic polarisation and corrosion of cemented carbides with cobalt and nickel binders. *J. Mater. Sci.*, **23** (1988) 914–18.
5. Tomlinson, W. J. & Ayers, N. J., Anodic polarisation and corrosion of WC–Co hardmetals containing small amounts of Cr_3C_2 and/or VC. *J. Mater. Sci.*, **24** (1989) 2348–54.
6. Human, A. M., Northrop, I. T., Luyckx, S. B. & James, M. N., A comparison between cemented carbides containing cobalt- and nickel-based binders. *J. Hard Mater.*, **2** (1991) 245–56.
7. Fernandes, P. J. L., Luyckx, S. B., Human, A. M. & Robinson, F. P. A., Does the cobalt mean free path affect the corrosion behaviour of WC–Co? *J. Hard Mater.*, **3** (1992) 185–94.
8. Masumoto, Y., Takechi, K. & Imasato, S., Corrosion resistance of cemented carbide. *Nippon Tungsten Rev.*, **19** (1986) 26–32.
9. Kny, E. & Schmid, L., New hardmetal alloys with improved erosion and corrosion resistance. *Int. J. Refr. Metals Hard Mater.*, **6** (1987) 145–8.
10. Bayoumi, A. E., Stewart, J. S. & Bailey, J. A., The effects of cemented carbide binder composition on tool wear encountered in surfacing green lumber. *Wood Fiber Sci.*, **20** (1988) 457–76.
11. Human, A. M., The corrosion of tungsten carbide based cemented carbides. Doctoral thesis, Technical University of Darmstadt, 1994.
12. Human, A. M. & Exner, H. E., Electrochemical behaviour of tungsten-carbide based hardmetals. *Proc. 5th Inter. Conf. on the Science of Hard Materials*, Hawaii, 1995, *Mater. Sci. & Engng* (1996) (in print).
13. Hellsing, M., High resolution microanalysis of binder phase in as sintered WC–Co cemented carbides. *Mater. Sci. Technol.*, **4** (1988) 824–9.
14. Exner, H. E., Quantitative description of microstructures by image analysis. In *Materials Science and Technology*, Vol. 2B, ed. E. Lifshin. VCH Verlag, Weinheim, 1994, pp. 281–350.
15. Human, A. M., The production of WC–Ni–Cr/Mo cemented carbides and their properties. MSc dissertation, University of the Witwatersrand, Johannesburg, 1991.
16. Human, A. M., Roebuck, B. & Exner, H. E., Electrochemical polarisation and corrosion behaviour of cobalt and Co(W,C) alloys in 1N sulphuric acid, *Mater. Sci. Engng* (submitted).
17. Roebuck, B. & Almond, E. A., The influence of composition, phase transformation and varying the relative f.c.c. and h.c.p. phase contents on the properties of dilute Co–W–C alloys. *Mater. Sci. Engng*, **66** (1984) 179–94.
18. Allen, C., Corrosion of galvanised steel in synthetic mine waters. *Br. Corros. J.*, **26** (1991) 93–100.
19. Spiegler, R., Schmauder, S. & Exner, H. E., Finite element modelling of the thermal residual stress distribution in a WC–10 wt%Co alloy. *J. Hard Mater.*, **3** (1992) 143–51.
20. Voorhies, J. D., Electrochemical and chemical corrosion of tungsten carbide (WC). *J. Electrochem. Soc.*, **119** (1972) 219–22.
21. Kaesche, H., *Metallic Corrosion*. NACE, Houston, 1985.